PREDICTING PERMANGANATE OXIDIZABLE CARBON WITH MID-INFRARED DIFFUSE REFLECTANCE SPECTROSCOPY ACROSS WISCONSIN SOILS

By

LOGAN BRICE

A Thesis

Submitted in partial fulfillment of the requirements of the degree

MASTER OF SCIENCE

IN

NATURAL RESOURCES – SOIL SCIENCE

College of Natural Resources

UNIVERSITY OF WISCONSIN

Stevens Point, Wisconsin

June, 2023

APPROVED BY THE GRADUATE COMMITTEE OF:

_____

Dr. Bryant C. Scharenbroch, Committee Chairman

Associate Professor of Soil & Waste Resources

_____

Dr. Daniel Keymer

Associate Professor of Soil & Waste Resources

_____

Dr. Paul McGinley

Director of the Center of Watershed Science and Education

TABLE OF CONTENTS

ABBREVIATIONS

IR, Infrared; MIR, diffuse reflectance Fourier transformed mid-infrared spectroscopy; PCA, principal components analysis; POXC, permanganate-oxidizable carbon; PLS, partial least squares; RMSE, root mean squared error; SOC, soil organic carbon; SOM, soil organic matter.

ABSTRACT

Labile carbon is a portion of soil organic matter (SOM) associated with biological activity and is commonly used as an indicator of soil health. Permanganate oxidizable carbon (POXC) has been proposed as an indicator of labile carbon that reflects a soil's response to management. Permanganate oxidizable carbon provides infield assessment of soil dynamics but relies upon uncertain assumptions related to the chemical composition of oxidized materials and methodological limitations restrict analysis to mineral soils. Rapid assessment and greater understanding of the oxidation reactions of labile fractions of SOM are needed to create a more robust soil health indicator. Recent applications of spectroscopy have demonstrated accurate measurements of SOM fractions with higher sample throughput than POXC. Advantages of spectroscopy include non-destructive analysis and prediction of multiple soil properties from a single spectral scan. This study focuses on predicting POXC with mid-infrared (MIR) diffuse reflectance spectroscopy and the identification of associated functional chemical groups. Spectral data from 710 soil samples were collected by an Agilent 4300 FTIR instrument. Predictive models were built using partial least squares (PLS) regression and performance was evaluated with R^2 and root mean square error (RMSE). Six models were built with an All-Soils model and five subsets based on SOM %. Utilizing the entire MIR spectral region, the All-Soils model had R^2 = 0.76/0.75 (Cal/Val) with RMSEC = 100.9 and RMSECV = 109.8 mg/kg POXC. The prediction of POXC in this model relied upon positive correlations with the following spectral peaks: 1,565 (amide II), 1,660 (amide I), 1,722 (carboxylic acid), 2,851 and 2,924 (aliphatic symmetric and anti-symmetric). The spectral peaks correlated with POXC prediction varied in other tested models as did SOM %. In general, the SOM

subset models gave inaccurate predictions, but revealed changes in the spectral peaks correlated with POXC prediction at certain SOM concentrations. The All-Soils model showed POXC prediction with a handheld MIR instrument can be accurate. There is a need for rapid and accurate quantification of soil health indicators, and we produced predictive models from an instrument applicable for in-field use.

ACKNOWLEDGEMENTS

My sincerest appreciation to Dr. Bryant Scharenbroch, my advisor, for finding me in a hoophouse of tomatoes and giving me the opportunity to dig into soil science research. He is an excellent mentor and friend, keeping my mind filled with ideas and freezer filled with roosters, and I am indebted to him for this.

I would like to wholeheartedly thank my graduate committee Dr. Daniel Keymer and Dr. Paul McGinley for their continued guidance and dedication which was crucial for the completion of this project. Their time and efforts are greatly appreciated, and their vast knowledge was instrumental to my personal educational development.

Additional thanks to all members of the UWSP pedology lab for their work preparing samples, collecting data, and brainstorming ideas together. Specifically, I am grateful for the friendship and contributions of Mark Cook in helping develop our protocol for POXC and Garrett Klepitsch for managing the acquisition of spectral data as well as trading R codes back and forth. I thank all members of the supporting Provisional Ecological Site Description research team including Dr. Jacob Prater, Joel Gebhard, and Shelly Stein for providing field descriptions and collecting the samples used in our project.

My gratitude goes to the Natural Resource Conservation Service for funding this research project and making this opportunity possible.

I thank my family for their continued loving support in my pursuit of educational advancement. To my parents for their unwavering dedication to cultivating my curiosity,

confidence, and commitment which were imperative to the successful completion of this project.

LIST OF TABLES

LIST OF FIGURES

INTRODUCTION

Permanganate oxidizable carbon (POXC) is thought to represent a stabilized, but slightly processed pool of labile soil organic matter (SOM) (Culman et al., 2012; Hurisso et al., 2016). Labile pools are a small but active fraction of SOM that are involved in the soil food web and influence biological and dynamic soil properties (Weil et al., 2003). Labile pools are characterized by rapid decomposition rates of weeks to years and compose 1-5% of total SOM (Scholes and Scholes, 1995). Cellular components of soil microbes such as carbohydrates, amino acids, peptides, amino sugars, and lipids are considered more labile fractions of SOM (Scholes and Scholes, 1995). These dynamic and active fractions of SOM are responsive to changes in the content of soil carbon and labile fractions are sensitive enough to show detectable differences from changes in soil carbon before a measurable response in total SOM (Gregorich and Janzen, 1996).

Measures of labile organic matter include particulate organic matter (POM) (Gregorich and Janzen, 1996), microbial biomass C (MBC) (Carter et al., 1999), potentially mineralizable carbon (PMC) (Zibiliske, 1994), and permanganate oxidizable C (POXC) (Weil et al., 2003). Particulate organic matter is a sand sized fraction of SOM that largely consists of undecomposed and partially decomposed plant residues (Marriott & Wander, 2006; Mirsky et al., 2008). Particulate organic matter fractionation by density yields a heavy (occluded) and light (free) fraction (Six et al., 1998). The light fraction is comprised of fresh roots and shoots residues residing between aggregates, while the heavy fraction consists of slightly decomposed residues and litter that are physically

protected within soil aggregates from additional degradation (Six et al., 1998; Wander 2004). Occluded POM commonly contains higher concentrations of C and N than free POM and proportionally contains a higher alkyl-C and lower O-alkyl-C content which may indicate a state of greater decomposition (Golchin et al., 1994a,b). Particulate organic matter methods vary based on fractionation by density or size which influence analytical values and associated interpretations (Culman et al., 2012).

Microbial biomass C is an estimate of C contained with soil microbes accounting for 1-3% of total soil organic C (Jenkinson 1987; Gregorich et al., 1994). Microbial biomass is involved in soil organic matter cycling and MBC can be a source or sink of labile C (Gregorich et al., 1994). Soil microbes are dynamic as they rapidly respond to changes in soil management or disturbance (Carter, 1986; Evangelou et al., 2020). Comparison of the ratio of MBC to total organic soil C allows for the assessment of organic matter dynamics (Gregorich et al., 1994). Monitoring changes in the ratio of MBC to total organic C can provide insight into organic matter additions into soil and conversion to MBC (Gregorich et al., 1994). Methods for measuring MBC include substrate induced respiration, chloroform fumigation-incubation, chloroform fumigation-extraction, and direct extraction by chloroform which commonly utilize a variable K_{ec} factor in quantification (Insam, 2001).

Potentially mineralizable C quantifies CO_2 generated after rewetting samples during a 1-3 day aerobic incubation (Franzluebbers, 1999). Franzlubbers (1999) showed a strong correlation between 24-day C mineralization of undisturbed soils and C mineralized in 3 days from dried and grounds samples that were rewetted. Methods for PMC usually measure the accumulation of CO_2 in an alkali trap but can also include

measuring CO_2 trapped in the headspace above incubating soils and use of automated electrolytic detectors or infrared gas analyzers (Gregorich et al., 1994). Quantifying PMC relies on the total amount of CO_2 released which is influenced by the duration of incubation, interval of CO_2 measurements, soil moisture content, room temperature, aeration, and sample pre-treatments such as drying (Gregorich et al., 1994). A lack of standardization in methodology makes comparisons of these soil properties between studies difficult.

Permanganate oxidizable carbon is an indirect measurement of a C pool assumed to be labile based on colorimetric quantification of permanganate reduction (Gruver, 2015). Loginow (1987) used permanganate to fractionate SOM under the assumption that 1 mol of permanganate oxidizes 0.75 mol (9000 mg) of C and microbial decomposition of SOM via oxidative enzymes may relate to the susceptibility of labile SOM fractions to oxidation via permanganate. Blair (1995) developed a labile soil C measurement based on oxidization with a standard concentration of permanganate for 1 hour. Weil et al., (2003) reduced the permanganate concentration used in soil oxidation to reduce safety concerns while handling the reagent, allowed the method to be employed in the field, and proposed a concept of labile C based on this modified method quantifying the amount of permanganate oxidation.

Permanganate oxidizable carbon has emerged as the routine and standard measure of labile SOM due to its practicality, accuracy, and correlation to other assessments of labile organic matter (Hurisso et al., 2016). Other methods (POM, MBC, and PMC) are

more costly compared to POXC. These other methods also required expensive and specialized equipment, such as a combustion analyzer or gas chromatograph to quantify soil C or carbon dioxide. Variations in methods for POM, MBC and PMC make interpretations and spatial and temporal comparisons difficult (Culman et al., 2012). In comparison, POXC methods are more standardized, require less specialized equipment, may be field adaptable (Weil et al., 2003). For these reasons, (POXC) is a consider a simple and rapid assessment of labile organic matter sensitive to the effects of management on soil C (Culman et al., 2012; Gruver 2015). Culman et al. (2012), reported POXC was as capable as POM and MBC in detecting the effects of management on soils. A stronger correlation between POXC and a more decomposed occluded POM suggests POXC is best at detecting differences in management practices that sequester carbon (Culman et al., 2012).

Permanganate oxidizable carbon (POXC) has been proposed as a soil health indicator. It can detect initial changes in soil properties resulting from alterations in management practices (Culman et al., 2012; Gruver 2015). The role of POXC as a labile soil health indicator is still debatable and needs further substantiation. Huang et al. (2021) reported POXC strongly correlated with SOC (R^2 of 0.84). Less than a 12% difference was found between the chemical properties of POXC and SOC suggesting a cage of covariance with these two properties (Huang et al., 2021). Lucas and Weil (2012) found that SOC and POXC were comparable in detecting changes in crop yields resulting from SOM management. Culman et al. (2013) demonstrated crop yield predictions from POXC were most influenced by more recalcitrant forms of carbon. Recalcitrant forms of

C including aromatic lignin can be more reactive with permanganate (MnO_4^-) than carbon forms such as cellulose that are considered labile (Tirol-Padre & Ladha, 2004; Skjemstad et al., 2006). Inorganic molecules containing Nitrogen and Sulfur can also be oxidized by MnO_4^- (Simandi et al., 1984; Song et al., 2017). These results challenge the connotation of POXC as a measurement of organic C oxidation associated with biological lability.

Permanganate oxidizable carbon has methodological limitations. For instance, challenges exist for quantification of the upper quantification threshold for POXC (Gruver, 2015). Current methods react 20 ml of a 20 mM permanganate (MnO_4^-) solution with 2.5g soil samples and determine organic matter oxidation indirectly from colorimetric measurement of MnO_4^- reduction. A maximum detection threshold of 1,440 mg kg^{-1} POXC occurs when all MnO_4- in solution is reduced. The upper limit of detection can be observed visually in "bleached" samples as the characteristic purple color of MnO_4^- turns clear once reduced. The SOM concentrations required to reach this threshold can vary due to the chemical composition of organic matter at certain stages of decomposition. Gruver (2015) found the current methods lack enough MnO_4^- to remain within the detection limits across the SOM contents found in agricultural soils. Wade et al. (2020) recommended analysis of samples with SOM < 10% to limit the number of results outside the detection threshold.

Permanganate oxidizable carbon (POXC) has limitations related to reaction rates that influence interpreted labile SOM pools (Gruver, 2015). A conveniently assumed linear relationship between POXC and SOM is used in calculating POXC with a maximum detection threshold of 1,440 mg kg^{-1} (Gruver, 2015). However, at certain concentrations of SOM the linearity of this relationship is not maintained as POXC

analysis becomes less sensitive in soils with more SOM due to their higher reducing potential of $KMnO_4$. Gruver (2015) proposed a correction factor be applied to POXC to address this nonlinearity and advised against process-based corrections until greater understandings are made concerning the cause of nonlinearity. Wade et al. (2021) explored strategies to overcome issues with detection limits by reacting samples on a standard SOC mass rather than total soil mass. Wade et al. (2021) found that using a fixed SOC mass produced more consistent quantities of MnO_4^- reduced but did not significantly alter the amount of MnO_4- reduced per unit of soil mass reacted. The additional time required to determine SOC prior to POXC analysis didn't provide a meaningful change to the number of results within the detection limits. However, variable ratios of MnO_4^- : SOC in reactions allow for variable rates of MnO_4^- reduction and inferred concentrations of oxidized SOM. Samples with higher SOC with have a lower ratio of MnO_4^- : SOC which supports lower oxidation rates and less oxidation of SOM pools. Therefore, this method will inherently measure different SOM pools with varying labile capabilities in samples with different amounts of SOM when using a fixed mass of soil reacted. While the proposed POXC method by Weil et al., 2003 is commonly used to assess labile C in the context of promoting soil health, questions remain regarding which soil compounds are oxidized in POXC reactions and variable rates of sample oxidation have been shown (Wade et al, 2021). A novel approach or new analytical tools are needed to address these methodological issues and associated interpretations.

The use of spectroscopic methods for measuring POXC might help alleviate some of the methodological challenges associated with traditional wet chemistry POXC determination. Infrared (IR) spectroscopy has been used to predict POXC, identify

organic functional groups, and assess changes in the abundance of those organic functional groups as SOM decomposes (Inbar et al., 1989; Chefetz et al., 1998; Calderón et al., 2017; Margenot et al., 2020; Huang et al., 2021). Mid-infrared spectroscopy (MIR) (400–4,000 cm^{-1}) detects fundamental molecular vibrations from many organic and mineral functional groups. The MIR fingerprint region (400-1,500 cm^{-1}) generally contains many spectral peaks that overlap and interfere with one another which makes functional group identification more challenging (Huang et al., 2021). The spectral signals in the MIR region, excluding the fingerprint, (1500–4,000 cm^{-1}) are often stronger than other IR regions making spectral peak identification and interpretations more straightforward (Calderón et al., 2017).

Spectroscopy provides additional advantages over conventional methods. Wet oxidation by MnO_4^- physically and chemically alters the sample beyond reconstitution which creates waste. Non-destructive MIR measurements preserve the sample allowing for multiple rescans. Spectral scans identify the fundamental chemical composition of a sample (Parikh et al., 2014). Spectral libraries containing spectral scans of many samples can be used to generate predictive models (Reeves et al., 2006). These models allow one scan of an unknown sample to predict many soil properties (Reeves et al., 2001). Sample preparation for MIR can be minimal to include only drying, although grinding can improve precision through homogenization.

Research of MIR predicted POXC have identified correlated spectral peaks associated with different functional chemical groups with recognizable chemical bonds. Calderón et al. (2017) reported primary peak assignments for POXC prediction as anti-symmetric and symmetric stretching of aliphatic C–H at 2,920 and 2,850 cm^{-1},

respectively. Margenot et al. (2020) and Huang et al. (2021) also ascribed stretches of aliphatic C-H at peaks between 2,925-2,930 and 2,850-2,852 cm^{-1} which correlated with POXC and SOC prediction. Negative correlations representing Si-O and quartz overtones were reported by both Margenot et al. (2020) and Huang et al. (2021) around 812 and 1,880 cm^{-1}, respectively. These mineral soil components had some of the strongest correlations with POXC prediction. Interference of carbonates can also occur between 2,925 and 2,850 cm^{-1} observed as shoulders with a corresponding peak at 2,520 cm^{-1}. In calcareous soils, acid treatment may be necessary to prevent interference that may otherwise overpredict SOM or POXC.

Spectral signatures distinct to POXC were isolated which may provide insights into what compounds undergo oxidation. Huang et al. (2021) used MIR photoacoustic spectroscopy, which offers less noisy spectral peaks in the fingerprint region, to isolate unique information to POXC. Regression coefficients of the partial least squares (PLS) regression models for SOC and POXC were determined on the whole MIR region. The regression coefficient of the POXC model was projected onto the regression coefficient of the SOC model to find the overlap in regression coefficients between the two models. The remaining portion of the regression coefficient of the POXC model is distinct to POXC (Huang et al., 2021). Isolated POXC spectral peaks included amide II at 1,574 cm^{-1}, aromatics at 1,495 cm^{-1} , polysaccharides at 1,138 cm^{-1} , and carbohydrates at 1,041 cm^{-1} (Huang et al., 2021).

The goal of this research is to determine if MIR can accurately predict POXC in 710 mineral soil samples representing the wide range of soils found throughout Wisconsin, USA. MIR models were generated across a gradient of SOM contents to test

the accuracy of POXC prediction in relation to changes in SOM. Spectral peaks associated with functional chemical groups were identified for each SOM model as those with the strongest correlations to POXC.

METHODS

Site Description and Field Sampling

This study included soils from twelve Major Land Resource Areas (MLRAs) and one hundred fifty-one Provisional Ecological Site Descriptions (PESDs) throughout Wisconsin, USA. Wisconsin PESD criteria included differences in organic or mineral soils, drainage classes, family textures, and other properties (e.g., carbonates, bedrock). Field plots (3-5) were sampled in each MLRA for each PESD. On each field plot, soils were described and classified to soil series following USDA-NRCS Soil Survey standard methods (Schoenberger and Wysocki, 2012; USDA-NRCS, 2017). Vegetation on each plot was sampled and quantified following standard protocols for Ecological Site Descriptions (USDA-NRCS, 2023).

In total, 615 pedons were described with 3,149 horizons sampled. These pedons included 254 series from 6 orders, 15 suborders, 32 great groups, and 84 subgroups. Soil samples were collected from each horizon, stored in wax-lined paper bags in a cooler, and returned to the laboratory for analysis and storage. In the laboratory, soil samples were air dried (20-22° C), sieved to <2 mm, ground with a mortar and pestle, and returned to wax-lined paper bags. Samples were stored at room temperature until further laboratory characterization. In total, 710 soil horizons were selected for this research of MIR prediction of POXC. Samples were randomly selected from sandy, loamy (fine loamy, coarse loamy, fine silty, coarse silty), and clayey (very fine and fine) texture classes based on family particle size classification. Five pedons from each of the 12 MLRAs were selected from each texture class. These samples include mineral soils with a SOM

range of 0.09 - 15.48 %. The sample set was comprised of 163 A horizons, 52 E horizons, 341 B horizons, and 154 C horizons.

Soil Sample Preparation

Prior to laboratory analysis, soil samples were ground using a Gilson 220V soil grinder with a 2mm sieve (Gilson Co., Lewis Center, OH). Most of this prepared sample was used for laboratory characterization, while the small portion used for MIR was ball-milled. A 15 cm^3 sub-sample was ground with a Vertical High Energy Planetary Ball Mill (MSE Supplies, Tucson, Arizona) prior to spectral analysis. The sample was ground in a 200 ml stainless steel jar containing 3mm, 5mm, and 12mm balls for 8 minutes at 1,028 RPM. This process ensures homogenization of samples while getting particle size to less than 200 microns.

Soil Organic Matter

Soil organic matter (SOM) was determined by loss on ignition (Sparks et al., 2020). Air-dried samples were placed in a muffle furnace for 6 hours at 450º C. The loss in sample mass after removal from the furnace is the result of SOM combustion. The percentage of air-dried mass lost in this process is the % SOM. Loss on ignition SOM was calculated with the following equation: SOM % = (air-dried soil weight (g) - post-ignition ash weight (g)) / air-dried soil weight (g) * 100

Permanganate-oxidizable C

Permanganate oxidizable carbon (POXC) analysis of mineral soils followed Weil et al. (2003) excluding a pH adjustment of the $KMnO_4$ solution as this has been shown to not alter POXC values (Gruver, 2015). All reactions were performed by one individual to

minimize introduced error as suggested by Wade et al. 2020. First, 18.0ml of deionized water was added to 50ml falcon tubes before the addition of 2.5g of soil. Next, 2.0ml of 0.2 M potassium permanganate/ 1.0 M calcium chloride solution was added to the falcon tubes before quickly capping and shaking by hand for 2 seconds. Reaction tubes were then placed on an Eberbach 6000 benchtop for 2 minutes. After 2 minutes, tubes were removed from the shaker table before being quickly shaken to remove soil from caps and allowed to settle for 10 minutes. Tubes were uncapped at this time while ensuring minimal movement and disturbance of reaction tubes. After settling, 0.5ml of solution was transferred to a falcon tube containing 49.5ml of DI water. Tubes were capped, inverted, and hand shaken for 5 seconds prior to absorbance analysis. Absorbance was determined using a ThermoScientific GENESTS 10S VIS spectrophotometer (Waltham, MA) at 550 nm. Reactions were performed in batches of 18 reaction tubes containing 6 untested samples in triplicate. Replicates were organized in series order. Stock solution standards were created with molarities of 0.005, 0.01, 0.015, and 0.02. POXC was determined from the following equation (a and b are y-int and slope from the standard curve):

POXC (mg kg^{-1}) = [0.02 mol/L - (a + b * absorbance)]*(9000 mg C/mol)*(0.02 L solution/0.0025 kg soil)

Mid-Infrared Spectroscopy

Spectral scans of samples were performed by a handheld Fourier Transform Infrared (FTIR) 4300 (Agilent Technologies, Santa Clara, CA) instrument with a diffuse reflectance probe. A 5ml scoop of sample was gently pressed, ensuring a level surface free of microtopography, into a vial cap for each spectral reading. Duplicate scans were

taken for each sample and samples were reloaded into vial caps for each reading. Background reference was set with a gold coin supplied by the manufacturer at the start of data collection and every 30 minutes afterward. This reference adjusts the handheld instrument if environmental conditions in the lab or field change while scanning. An instrument stand was used in the lab for scanning to minimize user interference on spectral signals. Once attached to the stand, the instrument was lowered until contact with the prepared sample was made. A fine-tuning knob and real-time display of spectra allowed for scans to be taken with reduced noise. Scans were taken with 8 background scans and 64 co-added scans spanning 4,000-650 cm^{-1} wavenumbers at intervals of about 2 cm^{-1} (yielding 1,798 data points for each sample).

Model Development and Statistical Analyses

Spectral processing and model development were performed using Microlab Expert and R-Studio Version 4.2.1 (Funny-Looking Kid), respectively. Two replicate scans of each sample were averaged and combined to create the spectra used for model development. Reflectance values of the averaged spectra were converted to absorbance ($\log^{10}(R)$). Pre-processing methods included baseline correction and smoothing. Baseline correction attempts to separate the spectra signals of actual functional groups from noise interferences or background effects. Smoothing (Savitzky-Golay algorithm Savitzky & Golay, 1964) serves to reduce noise on a single sample spectrum.

Principal component analyses (PCA) were performed on the processed spectral data. Principal component analysis reorganizes information from a large number of variables into a few variables called principal components that account for most of the variability in the data. This PCA transformed the roughly 1,800 spectral wavenumbers

into 10 principal components that contain most of that information. Calderón et al. (2017), used PCA to compare and separate land uses and site differences into spectral classes within the dataset. This approach was used for PLS regression model creation as well as analyses of spectral variability based on SOM classes.

Partial least squares (PLS) regression models were built with the pls package in R Studio using the full spectrum sample set with randomly selected 70% calibration and 30% validation sets. The number of components used was based on minimizing the difference between the root mean squared error (RMSE) of calibration and RMSE of cross-validation as well as the lowest reasonable RMSE of cross-validation. The initial model utilizing all 710 samples was built using the first 10 principal components and all subsequent models were created with 10 components.

Six models were built based on SOM to include an All-Soils, Very Low SOM, Low SOM, Medium SOM, High SOM, and Very High SOM models. The All-Soils model contained all 710 samples with SOM (0.09 - 15.48%). The Very Low SOM (0.09 - 0.749%) model contained 132 samples with the same calibration and validation designation as the All-Soils model. The Low SOM (0.75 - 1.49%) model contained 168 samples and the Medium SOM (1.5 - 2.49%) model had 136 samples. The High SOM (2.5 - 4.99%) model was built with 156 samples and the Very High SOM (5.0 - 15.48 %) model used the remaining 118 samples. The SOM breakpoints were selected to evenly distribute the number of samples within each model. These are arbitrary designations not related to SOM thresholds conceptualized for soil health. The six models were created and compared to assess correlations between the spectra and analytical SOM data. The coefficient of determination (r^2), root mean square errors and the regression coefficients

were used to assess model performance and also identify spectral peaks associated with POXC prediction. This approach identified which chemical groups are involved in POXC prediction for each SOM class.

RESULTS AND DISCUSSION

POXC and SOM data distributions

The sample distribution of SOM and POXC are displayed in Figure 1 and Figure 2, respectively. Average sample POXC and SOM values were 204.8 mg kg^{-1} and 2.83% within the dataset range of 1.1 - 1,173.6 mg kg^{-1} and 0.1 - 15.5%. The distribution of SOM was positively skewed as over 60% of samples had less than 2.5% SOM (Figure 1). The distribution of POXC was also positively skewed as over 70% of samples contained less than 200 mg kg^{-1} (Figure 2).

Although a greater number of samples had low values, the correlation between POXC and SOM was generally stronger as both values increased.

POXC correlation with SOM

The relationship between SOM and POXC is summarized in Figure 3 for each model. In the All-Soils model, POXC increased by around 69 mg kg^{-1} per 1% gain in SOM. A linear regression fitted to the dataset had an R^2 of 0.71 (Figure 3A). The All-Soils model had the strongest correlations between POXC and SOM, followed by the Very High SOM model (Figure 3F). The weakest correlation between POXC and SOM was observed in the Very Low SOM model (Figure 3B). The Low and Medium SOM models also had weak correlations between POXC and SOM, while the High SOM model showed a slightly higher correlation.

Model performance

The All-Soils model provided the most reliable predictions of POXC with calibration R^2 of 0.76 and validation R^2 of 0.75 (Table 2). The degree of error between the calibration (RMSE of 100.9) and validation (RMSE of 109.8) datasets was the smallest in the All-

Soils model (Table 2). The Very Low SOM model performed the poorest of the models tested with R^2 of calibration and validation both below 0.00005 (Table 2). The RSMEC of 17.5 and RMSECV of 50.7 were some of the lowest values of the models tested but were relatively high given the average POXC value in this model was 52.7 mg kg^{-1}. The calibration R^2 was higher than the validation R^2 in the Low and Medium SOM models (Table 2). The RMSEC was lower than RMSECV in both models. The two highest calibration R^2 were from the High and Very High SOM Models. Both models had RSMEC around 60 mg kg^{-1}, while RMSECV was almost three times that amount.

Spectral peaks associated with POXC

Regression coefficients of the All-Soils model allowed for the identification of spectral peaks important for the prediction of POXC (Figure 6). Only the regression coefficients from principal component 1 are shown in Figure 6. A summary of the correlated spectral peaks for each model can be found in Table 3. In the All-Soils model, the first component accounted for 54.77% of model variation and principal component 2 explained an additional 15.88%. Positive regression coefficients were observed at 1,565 cm^{-1} commonly assigned to Amide II with N-H bend and C=N stretch (Janik et al., 2007), 1,660 cm^{-1} attributed to C=O stretch (Amide I), 1,722 cm^{-1} ascribed as Carboxylic acid C=O stretch, 2,851 and 2,924 cm^{-1} accredited as aliphatic C-H symmetric and antisymmetric stretch, 3,086 cm^{-1} attributed to aromatic C-H stretch, and 3,296 cm^{-1} assigned to hydrogen bonded O-H and N-H stretch. Negative correlations can be seen at 1,876 cm^{-1} ascribed to quartz overtone and at 3,709 cm^{-1} which is associated with the stretching of inner-surface clay hydroxyl groups (Nguyen et al., 1991).

Regression coefficients of the Very Low SOM model can be found in Figure 6. Principal components 1 and 2 explained 48.96% and 26.85% of model variability, respectively. Positive correlations at 1,654, 2,817, and 3,628 cm^{-1} were observed. Negative correlations occurred at bands 1,808 and 2,537 cm^{-1}. The peak around 2,500 cm^{-1} can indicate the presence of carbonates. The Very Low SOM model was the only model with a negative correlation at 2,547 cm^{-1}.

The regression coefficients of the Low SOM model were most similar to the Very Low SOM model (Figure 6). Principal component 1 accounted for 44.18% and the second component 22.19% of model variation. Positive correlations were found at 1,645, 2,529, and 2,898 cm^{-1}. Negative correlations exist with the bands 1,889, 1,988 and 3,644 cm^{-1}. The peak around 1,988 cm^{-1} can be attributed to the same weak C-H bending of the aromatic overtone, found between 1,650 – 2,000 cm^{-1}.

The regression coefficients of the Medium SOM model are shown in Figure 6. The first principal component explained 51.74% of model variation, while the second component added 20.5%. The emergence of positive correlations at 1,546 and 1,561 cm^{-1} occurred in the Medium SOM (1.5 - 2.49%) model. Positive regression coefficients were also found at 1,697, 2,547, 2,847, and 2920 cm^{-1}. Negative correlations occurred as a sharp peak at 3,619 cm^{-1} and three subtle peaks around 1,890 cm^{-1}. There are similar correlations with the regression coefficients of the All-Soils and the Medium SOM models, but the magnitude of the regression coefficients of the All-Soils model was greater.

Regression coefficients of the first principal component for the High SOM model are found in Figure 6. Component 1 accounted for 61.9% of model variance and the

second component explained 9.34%. Positive correlations were at 1,580, 2,511, 2,603, 2,851, and 2,925 cm^{-1}. Negative correlations occurred at 1,882 and 3,631 cm^{-1}.

Regression coefficients from principal component 1 of the Very High SOM model are shown in Figure 6. This first component explained 62.58% of model variability, while component 2 accounted for 5.7%. Bands 1,547, 2,853 and 2,920 cm^{-1} were positively correlated with the Very High SOM model. Negative correlations can be seen at peaks 1,807 and 3,630 cm^{-1}.

Functional chemical groups important for the prediction of POXC across a range of SOM were found in the All-Soils model. Unique peaks were observed in various SOM models that relate to POXC prediction at certain concentrations of SOM. Throughout all tested SOM levels, correlations were observed with aliphatic C-H stretches (2,851 and 2,924), the inner-surface hydroxyl stretches of clays (3,619-3,709 cm^{-1}) and the quartz overtone (1,876 cm^{-1}). All models had positive correlations with the symmetric aliphatic C-H stretch around 2,850 cm^{-1}, however, the emergence of the anti-symmetric aliphatic C-H stretch (2,924 cm^{-1}) occurs in the Medium SOM model and carries to the Very High SOM. In this study, samples with less than 0.749% SOM and 250 mg kg^{-1} POXC had a positive correlation with the clay associated peak. All other tested models (0.75 - 15.5% SOM) had negative correlations with this clay peak. All models had a negative correlation with the quartz overtone with an increasingly negative regression coefficient as POXC and SOM increased. Four of the six models (Very Low, Low, Medium SOM, and All-Soils) had positive correlations with Amide I (1,645 – 1,697 cm^{-1}). In this study, the Amide I peak was positively correlated with POXC prediction in SOM models having less than 2.5% SOM and 500 mg kg^{-1} POXC. Lastly, the possible carbonate peak around

2,500 cm^{-1} was observed in all models. All models except for the Very Low SOM model had positive correlations with this carbonate peak. There is likely some interference occurring from the presence of this carbonate peak, however, there are counteracting correlations built into the All-Soils model. Any carbonate concerns could be alleviated by treating samples with acid prior to spectral analysis.

CONCLUSION

The PLS regression models built from analytical POXC and MIR spectral data have shown accurate POXC prediction across a range of SOM. The relatively poor performance of each SOM model may be due to relatively smaller sample sets (less than 170 each) representing a heterogeneous array of soils across the state of Wisconsin. When using smaller data sets, model performance may improve with the use of localized soil samples with similar characteristics, such as textures and mineralogy. The effect of SOM on POXC prediction was shown to influence the correlated spectral peaks, while the accuracy of all SOM subset models was low throughout. Organic samples were excluded from this study due to the commonly understood issues with detection limits. Still, there were issues with detection limits in the Very Low SOM model. The poor predictive performance as well as the presence of negative analytical POXC values in this SOM range indicate similar issues. Future work exploring low SOM samples may provide substantiation to these detection limit issues. However, the usefulness of POXC information on samples with less than 0.749% SOM may be as applicable as POXC on organic samples with excess SOM. The emergence of correlated spectral peaks at certain concentrations of SOM were explored and future work could continue to develop these relationships. Several labile and recalcitrant organic function groups are correlated with POXC prediction. Inorganic functional groups containing sulfur and nitrogen were also positively correlated with POXC prediction, while others relating to clay and sand were generally negatively correlated. While the oxidation of SOM with POXC may target labile and recalcitrant organic function groups, POXC may still be useful for detecting changes in soil properties from alterations to SOM management. Future work should

characterize the spectra of samples before undergoing permanganate oxidation and compare those with the spectra of samples after POXC reactions. This may serve to identify correlated functional groups involved in POXC reactions rather than correlated functional groups involved in PLSR MIR prediction of POXC. This research has shown that POXC prediction with MIR can be accurate. The use of MIR for rapid quantification of POXC may be an important breakthrough in the field of health assessment, especially if this methodology can be applied to in-field investigations. Our research utilized a handheld MIR in a laboratory setting to build reliable models that will then be implemented in the field for soil quality assessment. Future work will explore the potential of MIR prediction of POXC in the field.

REFERENCES

Blair, G.J. (1995). Soil carbon fractions based on their degree of oxidation and the development of a carbon management index for agricultural systems. Aust. J. Agric. Res. 46 1459 1466 https://doi-org.ezproxy.uwsp.edu/10.1071/AR9951459

Calderón, F. J., Reeves, J. B. I., Collins, H. P., & Paul, E. A. (2011). Chemical Differences in Soil Organic Matter Fractions Determined by Diffuse-Reflectance Mid-Infrared Spectroscopy. Soil Science Society of America Journal, 75(2), 568–579.

Calderón, F. J., Culman, S., Six, J., Franzluebbers, A. J., Schipanski, M., Beniston, J., Grandy, S., & Kong, A. Y. Y. (2017). Quantification of soil permanganate Oxidizable C (POXC) using infrared spectroscopy. Soil Science Society of America Journal, 81, 277–288. https://doi.org/10.2136/sssaj2016.07.0216

Carter, M. R. (1986). Microbial biomass as an index for tillage-induced changes in soil biological properties. Soil Tillage Res.-7: 29-40.

Carter, M. R., Gregorich, E. G., Angers, D. A., Beare, M. H., Sparling, G. P., Wardle, D. A., & Voroney, R. P. (1999). Interpretation of microbial biomass measurements for soil quality assessment in humid temperate regions. Canadian Journal of Soil Science 79: 507–20. doi:10.4141/S99-012

Chefetz, B., Adani, F., Genevini, P., Tambone, F., Hadar, Y., & Chen, Y. (1998). Humic-acid transformation during composting of municipal solid waste. J Environ Qual. 27:794-800.

Culman, S., Snapp, S. S., Freeman, M. A., Schipanski, M. E., Beniston, J., Lal, R., Drinkwater, L. E., Franzluebbers, A. J., Glover, J. D., Grandy, A. S., Lee, J., Six, J., Maul, J. E., Mirksy, S. B., Spargo, J. T., &Wander, M. M. (2012). Permanganate Oxidizable Carbon Reflects a Processed Soil Fraction that is Sensitive to Management. Soil Science Society of America Journal, 76(2), 494–504. https://doi.org/10.2136/sssaj2011.0286

Culman, S. W., Snapp, S. S., Green, J. M., & Gentry, L. E. (2013). Short- and Long-Term Labile Soil Carbon and Nitrogen Dynamics Reflect Management and Predict Corn Agronomic Performance. Agronomy Journal, 105(2), 493–502. https://doi.org/10.2134/agronj2012.0382

Evangelou, E., Tsadilas, C., & Giourga, C. (2021). Seasonal Variation of Soil Microbial Biomass Carbon and Nitrogen as Affected by Land Use in a Mediterranean Agro Ecosystem. Communications in Soil Science and Plant Analysis, 52(3), 222–234. https://doi.org/10.1080/00103624.2020.1854298

Franzluebbers, A. J. (1999). Potential C and N mineralization and microbial biomass from intact and increasingly disturbed soils of varying texture. Soil Biol. Biochem., 31: 1083–1090.

Golchin, A., Oades, J. M., Skjemstad, J. O., & Clarke, P. (1994a). Soil structure and carbon cycling. Soil Research, 32(5), 1043-1068.

Golchin, A., Oades, J. M., Skjemstad, J. O., & Clarke, P. (1994b). Study of free and occluded particulate organic matter in soils by solid state 13C CP/MAS NMR spectroscopy and scanning electron microscopy. Soil Research, 32(2), 285-309.

Gregorich, E., Carter, M., Angers, D., Monreal, C., & Ellert, B. (1994). Towards a minimum data set to assess soil organic matter quality in agricultural soils. Canadian Journal of Soil Science, 74(4), 367–385. https://doi.org/10.4141/cjss94-051

Gregorich, E. G., & Janzen, H.H. (1996). Storage of soil carbon in the light fraction and macro-organic matter. In Advances in soil science: Structure and organic matter storage in agricultural soils, ed. M. R. Carter and B. A. Stewart, 167–90. Boca Raton, FL: CRC Press.

Gruver, J. (2015). Evaluating the Sensitivity and Linearity of a Permanganate-Oxidizable Carbon Method. Communications in Soil Science and Plant Analysis, 46(4), 490–510. https://doi.org/10.1080/00103624.2014.997387

Huang, J., Rinnan, Å., Bruun, T. B., Engedal, T., & Bruun, S. (2021). Identifying the fingerprint of permanganate oxidizable carbon as a measure of labile soil organic carbon using Fourier transform mid-infrared photoacoustic spectroscopy. European Journal of Soil Science, 72(4), 1831–1841. https://doi.org/10.1111/ejss.13085

Hurisso, T. T., Culman, S. W., Horwath, W. R., Wade, J., Cass, D., Beniston, J. W., Bowles, T. M., Grandy, A. S., Franzluebbers, A. J., Schipanski, M. E., Lucas, S. T., & Ugarte, C. M. (2016). Comparison of Permanganate-Oxidizable Carbon and Mineralizable Carbon for Assessment of Organic Matter Stabilization and Mineralization. Soil Science Society of America Journal, 80(5), 1352–1364. https://doi.org/10.2136/sssaj2016.04.0106

Inbar, Y., Chen, Y., & Hadar, Y. (1989). Solid-state carbon 13 nuclear magnetic resonance and infrared spectroscopy of composted organic matter. SSSAJ. 53:1695-1701.

Insam, H. (2001). Developments in soil microbiology since the mid 1960s. Geoderma, 100(3), 389–402. https://doi.org/10.1016/S0016-7061(01)00029-5

Janik, L. J., Skjemstad, J. O., Shepherd, K. D., & Spouncer, L. R. (2007). The prediction of soil carbon fractions using mid-infrared-partial least square analysis. Australian Journal of Soil Research, 45, 73–81. https://doi.org/10.1071/SR06083

Jenkinson, D. S. (1987). Determination of microbial biomass carbon and nitrogen in soil. Pages 368-386 in J. R. Wilson, ed. Advances in nitrogen cycling in agricultural ecosystems' CAB International, Wallingford, U.K.

Lucas, S., & Weil, R. (2012). Can a Labile Carbon Test be Used to Predict Crop Responses to Improve Soil Organic Matter Management. Agronomy Journal, 104(4), 1160–1170. https://doi.org/10.2134/agronj2011.0415

Margenot, A., O' Neill, T., Sommer, R., & Akella, V. (2020). Predicting soil permanganate oxidizable carbon (POXC) by coupling DRIFT spectroscopy and artificial neural networks (ANN). Computers and Electronics in Agriculture, 168(105098), 105098. https://doi-org.ezproxy.uwsp.edu/10.1016/j.compag.2019.105098

Marriott, E. E., & Wander, M. M. (2006). Total and Labile Soil Organic Matter in Organic and Conventional Farming Systems. Soil Science Society of America Journal, 70(3), 950–959. https://doi.org/10.2136/sssaj2005.0241

Mirsky, S., Lanyon, L., & Needelman, B. (2008). Evaluating Soil Management Using Particulate and Chemically Labile Soil Organic Matter Fractions. Soil Science Society of America Journal, 72(1), 180–185. https://doi.org/10.2136/sssaj2005.0279

Nguyen, T.T., Janik, L.J., & Raupach, M. (1991). Diffuse reflectance infraredFourier-transform drift- Spectroscopy in soil studies. Aust. J. Soil Res. 29:49–67. doi:10.1071/SR9910049https://doi.org/10.1016/j.soilbio.2019.107692

Parikh, S.J., Goyne, K.W., Margenot, A.J., Mukome, F.N.D., & Calderón, F.J. (2014). Soil chemical insights provided through vibrational spectroscopy. Adv. Agron. 126:1–148. doi:10.1016/B978-0-12-800132-5.00001-8

Reeves, J. B., McCarty, G. W., & Reeves, V. B. (2001). Mid-infrared Diffuse Reflectance Spectroscopy for the Quantitative Analysis of Agricultural Soils. Journal of Agricultural and Food Chemistry, 49(2), 766–772. https://doi.org/10.1021/jf0011283

Reeves, J.B., Follett, R.F., McCarty, G.W., & Kimble, J.M. (2006). Can near or mid-infrared diffuse reflectance spectroscopy be used to determine soil carbon pools? Commun. Soil Sci. Plant Anal. 37:2307–2325. doi:10.1080/00103620600819461

Savitzky, A., & Golay, M. J. (1964). Smoothing and differentiation of data by simplified least squares procedures. Analytical chemistry, 36(8), 1627-1639.

Schoeneberger, P. J., Wysocki, D. A., & Benham, E. C. (2012). Field book for describing and sampling soils / P. J. Schoeneberger, D. A. Wysocki, E. C. Benham. (P. J. Schoeneberger, D. A. Wysocki, & E. C. Benham, Eds.; Version 3.0.). National

Soil Survey Center, Natural Resources Conservation Service, U.S. Department of Agriculture.

Scholes, R.J., & Scholes, M.C., (1995). The effect of land use on nonliving organic matter in the soil. p. 210– 225. In R.G. Zepp and C. Sonntag (ed.) The role of nonliving organic matter in the earth's C cycle. John Wiley & Sons, Chichester, UK.

Simandi, L. I., Jaky, M., & Schelly, Z. A. (1984). Short-lived manganate(VI) and manganate(V) intermediates in the permanganate oxidation of sulfite ion. Journal of the American Chemical Society, 106(22), 6866–6867. https://doi.org/10.1021/ja00334a079

Six, J., Elliott, E. T., Paustian, K., & Doran, J. W. (1998). Aggregation and soil organic matter accumulation in cultivated and native grassland soils. Soil Science Society of America Journal, 62(5), 1367–1377. https://doi.org/10.2136/sssaj1998.03615995006200050032x

Skjemstad, J. O., Swift, R.S., & McGowan, J.A. (2006). Comparison of the particulate organic carbon and permanganate oxidation methods for estimating labile soil organic carbon. Australian Journal of Soil Research 44 (3): 255–63. doi:10.1071/SR05124

Song, Y., Jiang, J., Ma, J., Pang, S.Y., Luo, C., & Qin, W. (2017). Oxidation of inorganic compounds by aqueous permanganate: Kinetics and initial electron transfer steps. Separation and Purification Technology, 183, 350-357.

Sparks, D. L., Page, A. L., Helmke, P. A., & Loeppert, R. H. (Eds.). (2020). Methods of soil analysis, part 3: Chemical methods (Vol. 14). John Wiley & Sons.

Tirol-Padre, A., & Ladha, J. K. (2004). Assessing the reliability of permanganate-oxidizable carbon as an index of soil labile carbon. Soil Science Society of America Journal, 68(3), 969-978.

United States Department of Agriculture. Natural Resources Conservation Service. (2017). Soil survey manual. Agricultural Handbook 18. U.S. Department of Agriculture, Natural Resource Conservation Service, Washington, D.C

Wade, J., Maltais-Landry, G., Lucas, D. E., Bongiorno, G., Bowles, T. M., Calderón, F. J., Culman, S. W., Daughtridge, R., Ernakovich, J. G., Fonte, S. J., Giang, D., Herman, B. L., Guan, L., Jastrow, J. D., Loh, B. H., Kelly, C., Mann, M. E., Matamala, R., Miernicki, E. A., … Margenot, A. J. (2020). Assessing the sensitivity and repeatability of permanganate oxidizable carbon as a soil health metric: An interlab comparison across soils. Geoderma, 366(C), 114235–. https://doi.org/10.1016/j.geoderma.2020.114235

Wade, J., Li, C., Pulleman, M. M., Trankina, G., Wills, S. A., & Margenot, A. J. (2021). To standardize by mass of soil or organic carbon? A comparison of permanganate oxidizable carbon (POXC) assay methods. Geoderma, 404, 115392–. https://doi.org/10.1016/j.geoderma.2021.115392

Wander, M. (2004). Soil organic matter fractions and their relevance to soil function. p. 67– 102. In F. Magdoff, and R.R. Weil (ed.) Soil organic matter in sustainable agriculture. CRC Press, Boca Raton, FL.

Weil, R.R., Islam, K.R., Stine, M.A., Gruver, J.B., & Samson-Liebig, S.E. (2003). Estimating active carbon for soil quality assessment: A simplified method for laboratory and field use. Am. J. Altern. Agric. 18:3–17. doi:10.1079/AJAA2003003

Zibiliske, L. M. (1994). Carbon mineralization. In Methods of soil analysis, part 2: Microbiological and biochemical properties, ed. R. W. Weaver, S. Angle, P. Bottomly, D. Bezdicek, S. Smith, A. Tabatabai, and A. Wollum, 835–63. Madison, WI: SSSA.

APPENDIX

TABLES

TABLE 1. Summary of mid-infrared spectroscopy prediction of permanganate oxidizable carbon in the relevant literature. Includes cited authors of the research, the correlated spectral peaks for the model, partial least squares regression model performance metrics for calibration (Cal)/validation (Val) sets, and unique information from the study.

Authors	Spectral Peaks (cm^{-1})	Model Performance	Additional Information
Calderón et al. 2017 [a]	2,930 - 2,850 (aliphatic C-H stretch)	R^2 = 0.81/0.8; RMSE = 145.1/146.6; n = 496	Restricted data to samples w/ less than 4.6% SOC. Used hyperbolic fit regression for POXC and SOC.
Margenot et al. 2020 [b]	3,650 (phyllosilicate O-H); 2,920 (aliphatic C-H); 1,880 (quartz overtone); 818 (Si-O)	Cal R^2 = 0.75; RMSEC = 106; n = 144	Spectral scans spanned mid and near-infrared regions (8000 – 600 cm^{-1}). POXC composition may be influenced by mineralogy.

Huang et al. 2021 [c]	2,930 - 2,850 (aliphatic C-H stretch); 1,574 (amide II); 1,495 (aromatics); 1,138 (polysaccharides); 1,041 (carbohydrates)	R^2 = 0.854/0.848; RMSE = 121/123; n = 575 (removed 19 outliers)	POXC prediction is mainly based on correlations with SOC and little information unique to POXC exists. Identified 4 unique POXC peaks near and in the MIR fingerprint region.

Note. **[a] Pike AutoDIff diffuse reflectance accessory in line with Digilab FTS 7000 spectrometer. KBr beam splitter and deuterated triglycine sulfate detector. Spectra with 64 co-added scans produced 1868 data points at a resolution of around 2 cm^{-1} . Dataset split evenly with 50% as calibration and 50% as validation set.**

[b] Tensor 27 HTS-XT Bruker spectrometer. 80% of dataset used as calibration set with 20% as validation set.

[c] PA301 photoacoustic Gasera detector connected to a ThermoScientific Nicolet 6700 FTIR spectrometer. Spectrum. 64 scans at a resolution of 4 cm^{-1}.

TABLE 2. Performance metrics of each partial least squares regression model for the prediction of POXC from mid-infrared spectra. Includes statistics for the calibration and validation sets.

Model	Calibration			Validation		
	n	R^2	RMSEC	n	R^2	RMSEC
All_SOM	498	0.76	100.9	212	0.75	109.8
VLow_SOM	92	8.7E-06	17.5	40	1.8E-05	50.7
Low_SOM	118	0.61	30.4	50	0.17	47.7
Medium_SOM	97	0.67	73.9	41	0.14	120
High_SOM	109	0.84	61.3	47	0.3	151.1
VHigh_SOM	81	0.91	60.8	35	0.44	187.5

TABLE 3. Spectral peaks correlated with POXC prediction for each partial least squares regression model. (+) indicates a positive correlation and (-) signifies a negative correlation.

Model	Amide II (1,565 cm^{-1})	Amide I (1,660 cm^{-1})	Carboxylic acid (1,722 cm^{-1})	Quartz overtone (1,876 cm^{-1})	$CaCO_3$ (2,551 cm^{-1})	Alkane (2,851 cm^{-1})	Alkane (2,924 cm^{-1})	Clay hydroxyl (3,709 cm^{-1})
All-Soils	+	+	+	-	+	+	+	-
Very Low SOM		+		-	-	+		+
Low SOM		+		-	+	+		-
Medium SOM	+	+	+	-	+	+	+	-
High SOM	+			-	+	+	+	-
Very High SOM	+			-	+	+	+	-

FIGURES

FIGURE 1. Histogram of soil organic matter (SOM) %.

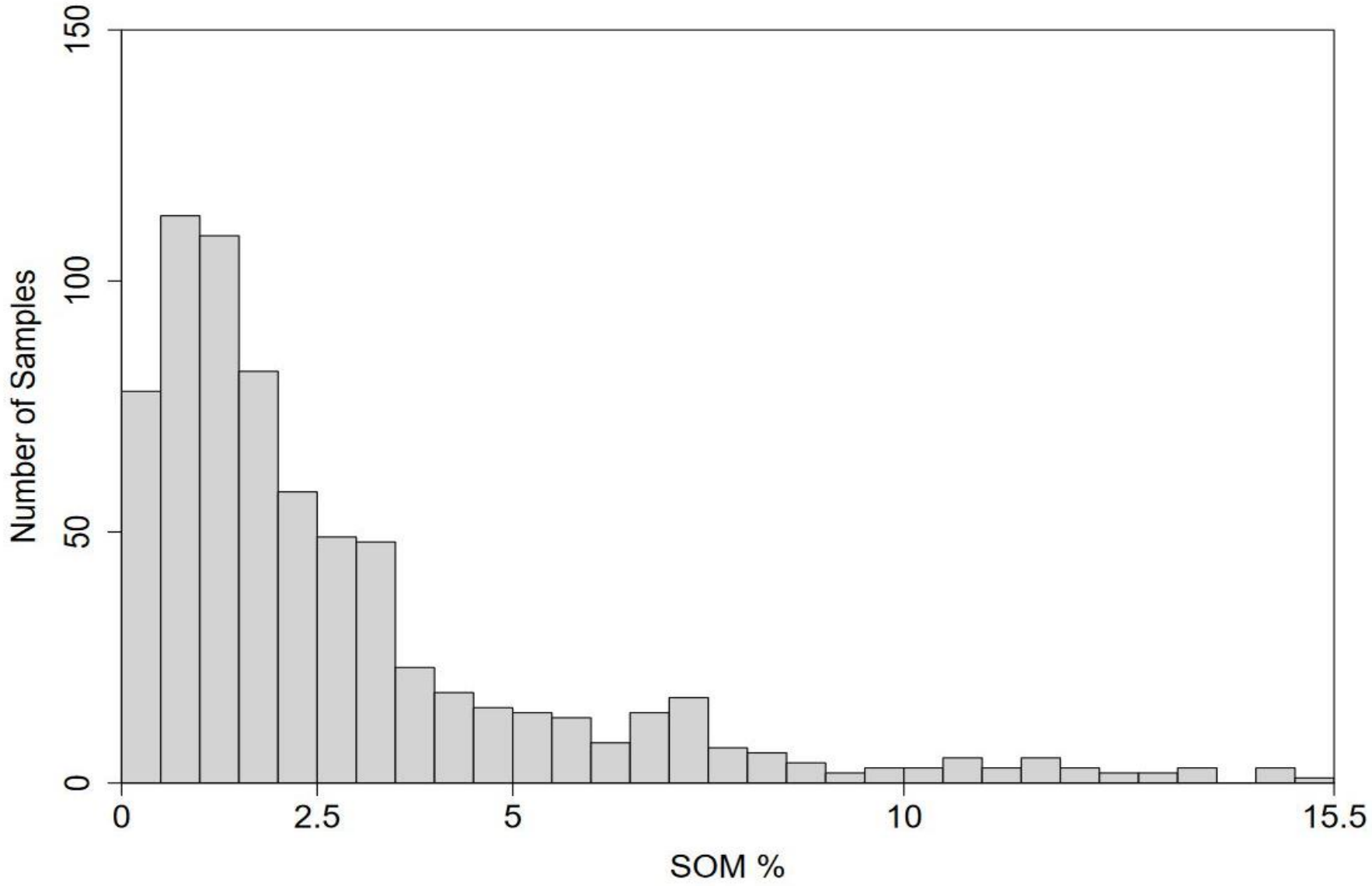

FIGURE 2. Histogram of permanganate oxidizable carbon (POXC).

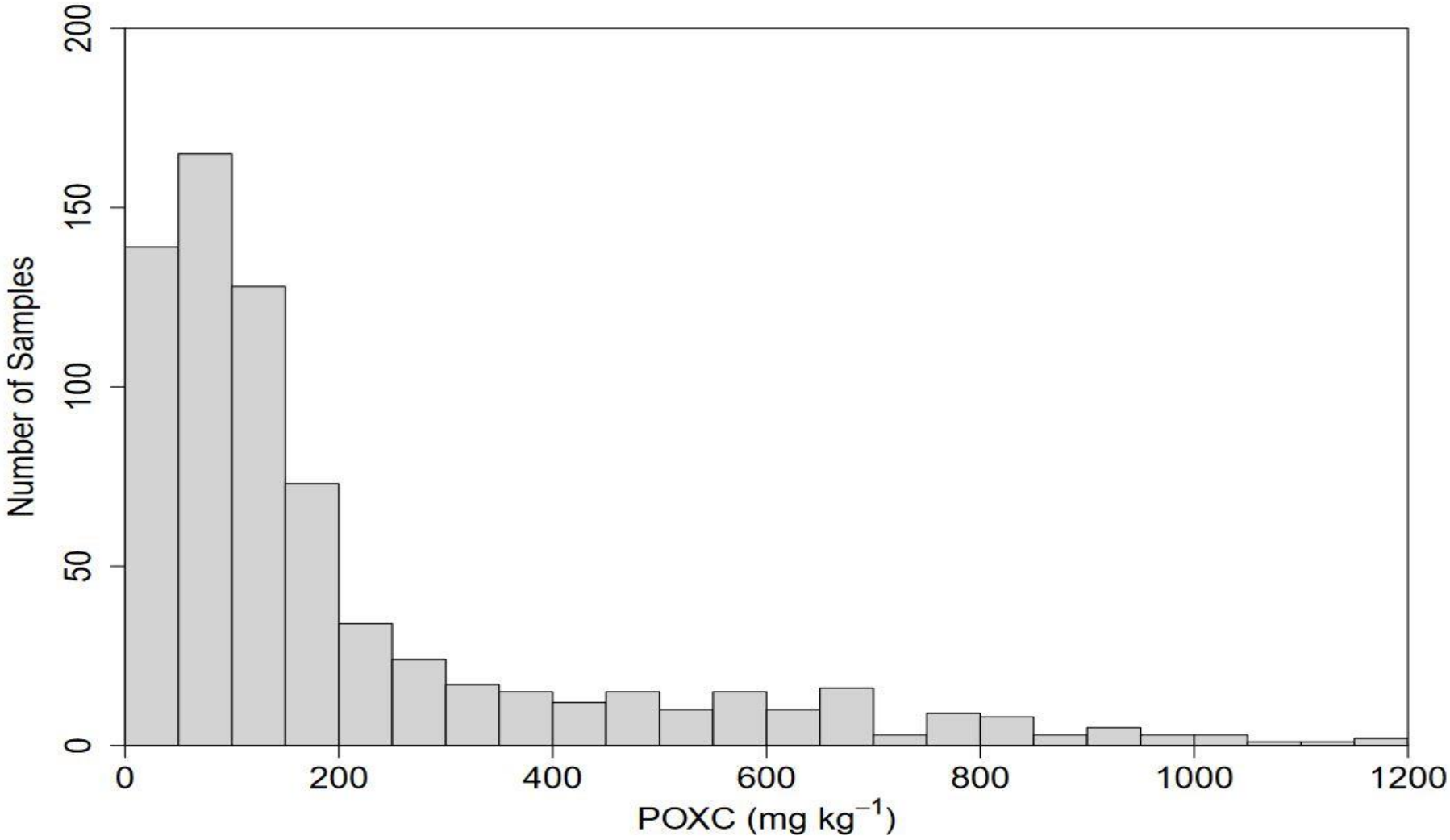

FIGURE 3. Linear fit regression of soil organic matter (SOM) and permanganate oxidizable carbon (POXC) for the All-Soils Model (A), Very Low SOM Model (B), Low SOM Model (C), Medium SOM Model (D), High SOM Model (E), and Very High SOM Model (F). The linear regression for each model can be seen as dashed black lines.

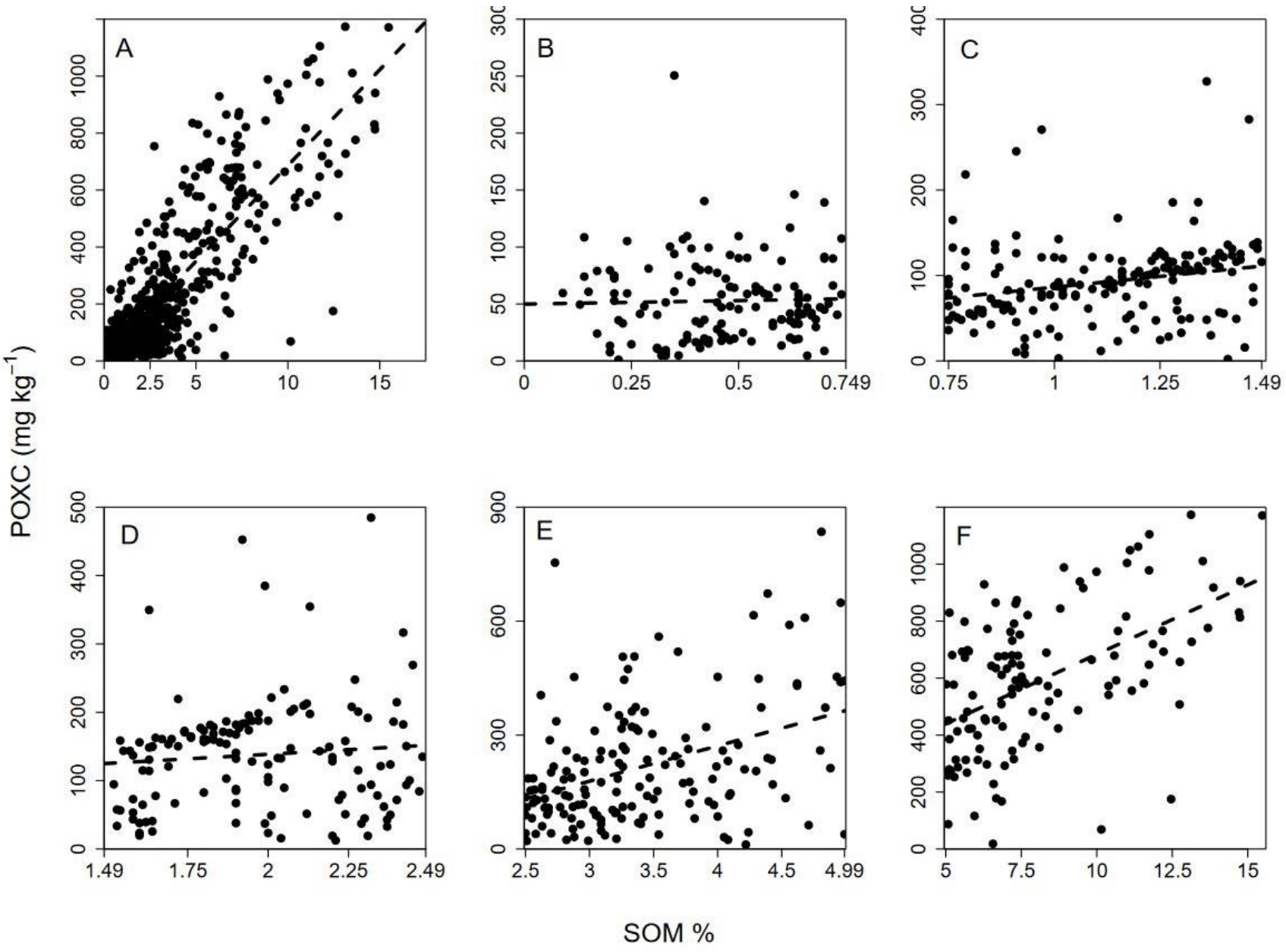
A
B
C
D
E
F
POXC (mg kg^{-1})
SOM %

FIGURE 4. Partial least squares regression predicted permanganate oxidizable carbon (POXC) vs. analytical actual POXC values for calibration (black dots) and validation (white dots) of mid-infrared models: All-Soils (A), Very Low SOM (B), Low SOM (C), Medium SOM (D), High SOM (E), and Very High SOM (F). The linear regression of calibration sets (solid line) and validation sets (dashed line) are shown for each model.

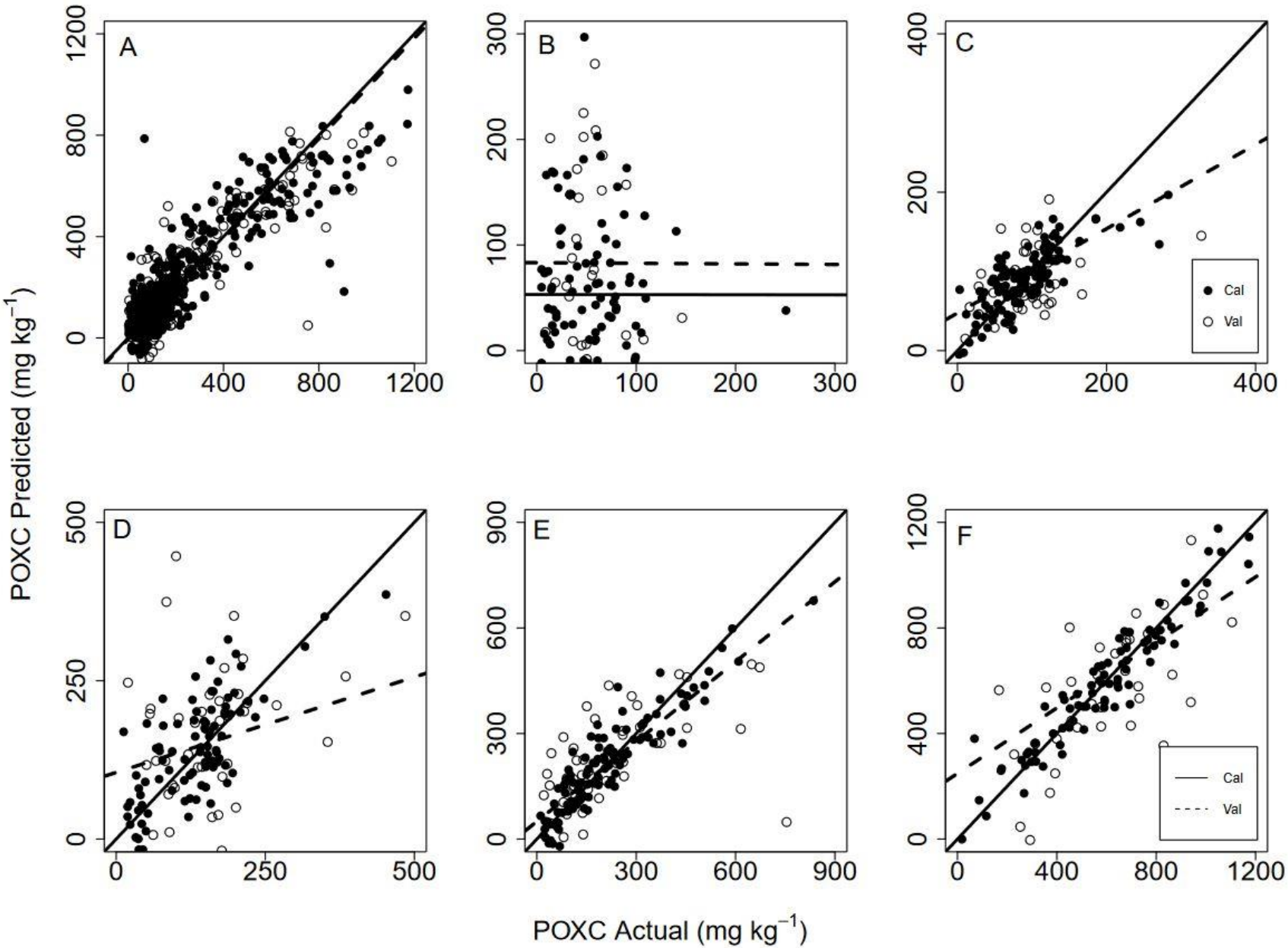
A
B
C
D
E
F
Cal
Val
POXC Predicted (mg kg^{-1})
POXC Actual (mg kg^{-1})

FIGURE 5. Diffuse reflectance Fourier transform mid-infrared average spectra for each partial least squares regression model. The legend code is as follows: All = All-Soils Model, VLow = Very Low SOM Model, Low = Low SOM Model, Medium = Medium SOM Model, High = High SOM Model, and VHigh =Very High SOM Model.

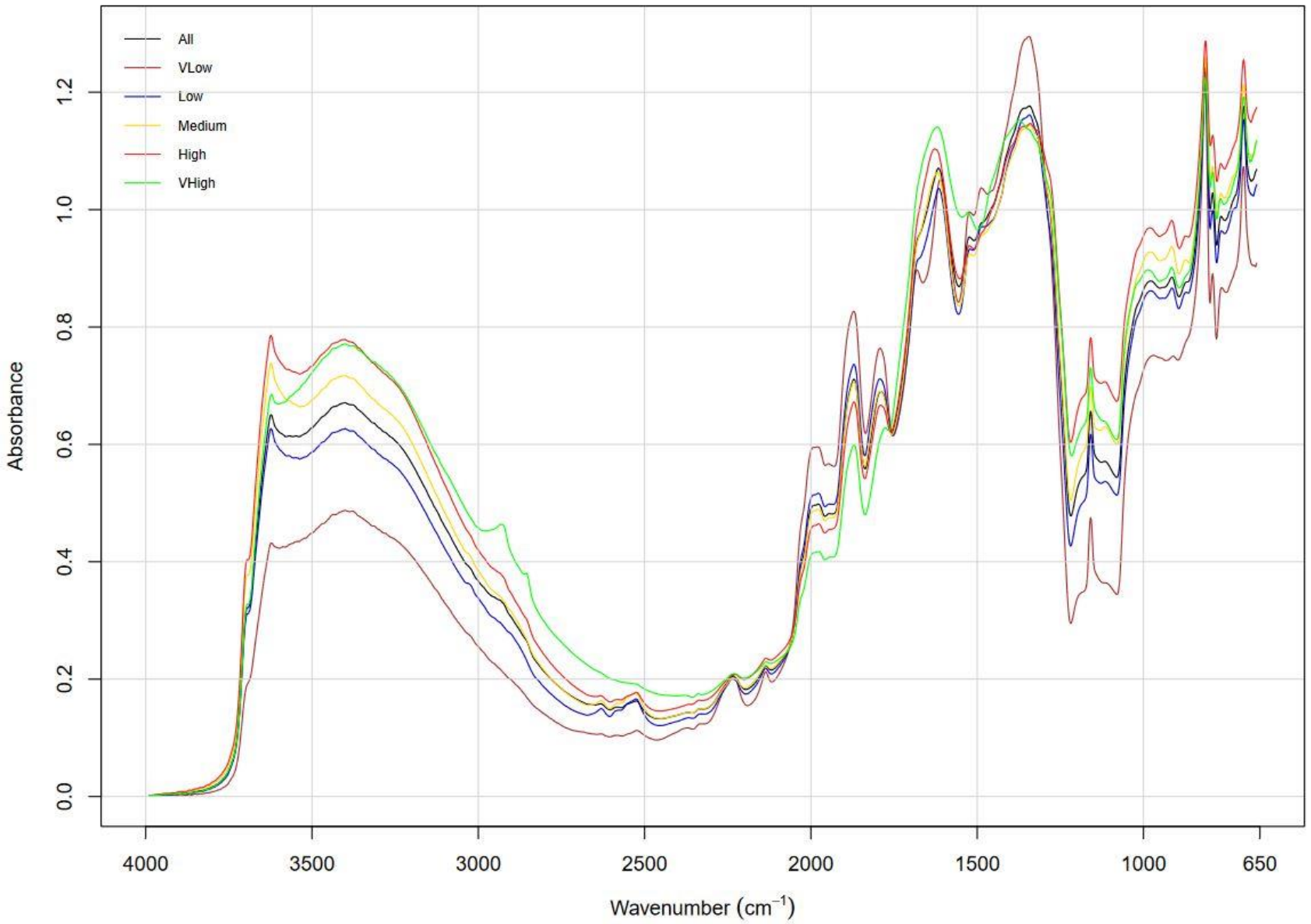
All
VLow
Low
Medium
High
VHigh
Absorbance
0.0
0.2
0.4
0.6
0.8
1.0
1.2
4000
3500
3000
2500
2000
1500
1000
650
Wavenumber (cm^{-1})

FIGURE 6. Regression coefficients of specific spectral peaks correlated with permanganate oxidizable carbon (POXC). The following models are displayed: All-Soils Model (A), Very Low SOM Model (B), Low SOM Model (C), Medium SOM Model (D), High SOM Model (E), and Very High SOM Model (F).

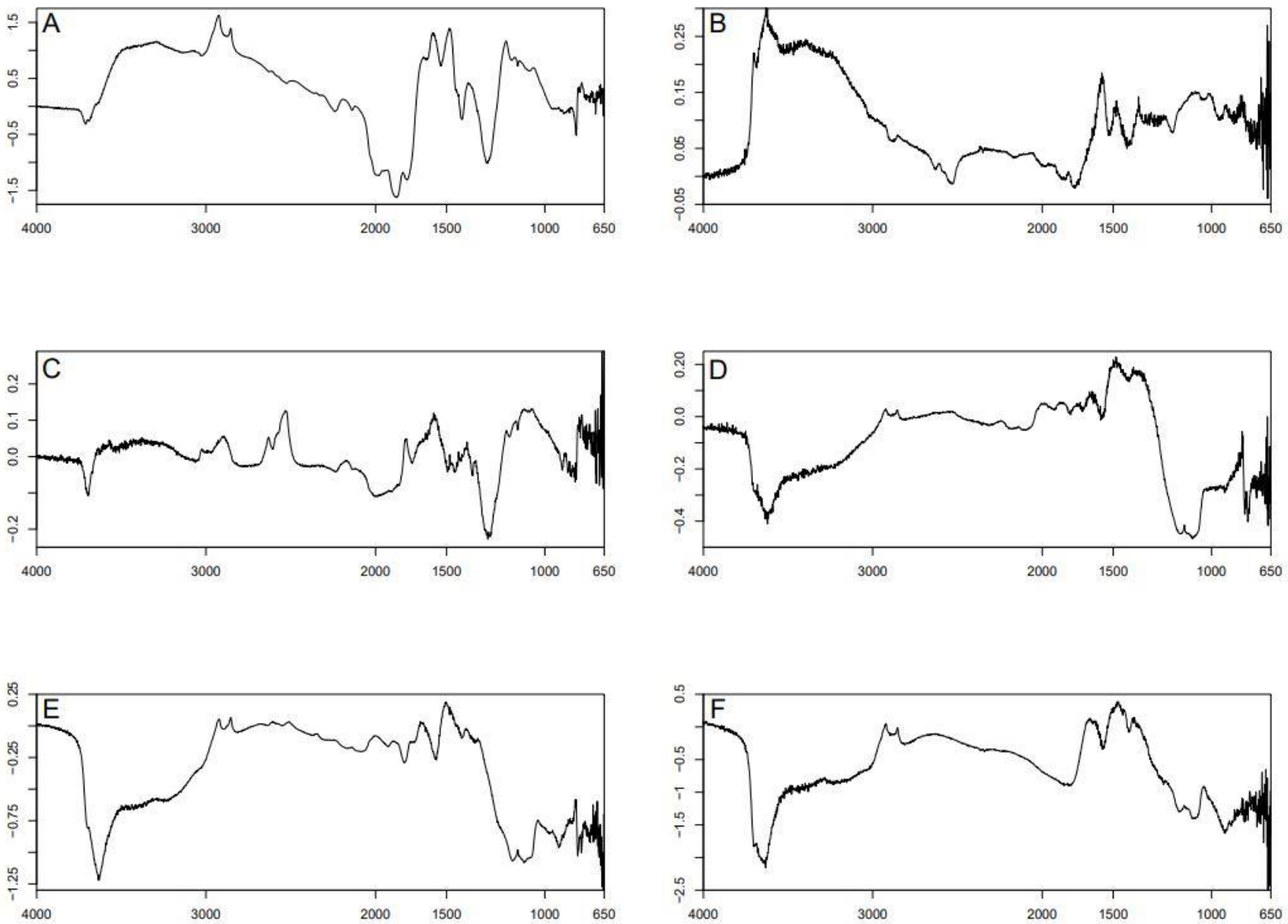
A
1.5
0.5
−0.5
−1.5
4000
3000
2000
1500
1000
650
B
0.25
0.15
0.05
−0.05
4000
3000
2000
1500
1000
650
C
0.2
0.1
0.0
−0.2
4000
3000
2000
1500
1000
650
D
0.20
0.0
−0.2
−0.4
4000
3000
2000
1500
1000
650
E
0.25
−0.25
−0.75
−1.25
4000
3000
2000
1500
1000
650
F
0.5
−0.5
−1
−1.5
−2.5
4000
3000
2000
1500
1000
650